Materials Science-Poland, *Vol. 28*, *No. 1*, *2010*

Characterization of electrochemically deposited thin Mo–O–C–Se film layers

N. DUKSTIENE[1*], L. TATARISKINAITE[2], M. ANDRULEVICIUS[3]

[1]Department of Physical Chemistry, Kaunas University of Technology, LT-50254 Radvilenu pl. 19, Kaunas, Lithuania

[2]AB Achema, LT-55550, Jonavos r., Ruklos sen., Jonalaukio k., Lithuania

[3]Institute of Physical Electronics of Kaunas University of Technology, LT-50131 Savanoriu pr. 271 Kaunas, Lithuania

The paper reports on the composition, morphology and optical properties of thin Mo–O–C–Se film electrodeposited onto SnO_2–glass substrate (R = 292 Ω/cm^2). The composition of films was estimated based on X-ray photoelectron spectroscopy and Fourier transform infrared spectral analysis. Structural elements similar to molybdenum oxides and/or hydroxides, $MoSe_2$, Se and SeO_2 were identified on the surface and in the bulk of the electrodeposits. The studies of surface morphology by scanning electron microscopy and atomic force microscopy showed long-sized wires distributed over all the surface. The optical absorption studies revealed the films to be highly absorptive ($10^4\alpha$ cm^{-1}) with a direct band transition and the bang gap energy of 1.75 eV.

Keywords: *thin film electrodeposition; XPS; $MoSe_2$; selenium; molybdenum oxides and hydroxides; optical properties*

1. Introduction

A rapid progress in modern technologies induces the search for new compounds possessing advanced physicochemical properties. Thin films of molybdenum chalcogenide and oxide based compounds present considerable interest for many research fields including electrocatalysis [1, 2], fuel cells [3] and batteries [4]. This interest is related to the capacity of Mo atoms to assume various oxidation states, depending on the methods of syntheses. Therefore, there is continuous research into exploring new processing techniques which fulfil low-cost, scalability and production criteria. Electrodeposition satisfies all these conditions and hence accelerated efforts are made in

[*]Corresponding author, e-mail: nijole.dukstiene@ktu,lt

many laboratories [4–6]. Thin amorphous MoO_yS_x films, applied in lithium battery cells, have been successfully obtained by the electrodeposition technique [4]. The cathodic deposition of complex Mo_4O_{11}–MoS_2 systems has been described in the paper [5].

Results regarding simultaneous electrodeposition of Mo and Se onto SnO_2 coated glass electrodes from sodium citrate solutions have been recently reported [6]. Mirror-like, uniform and adhesive thin Mo–O–C–Se films were electrodeposited on the surface of SnO_2–glass electrode. However it was impossible to characterize the crystallographic structures of the deposits: the only lines corresponding to polycrystalline SnO_2 have been observed in X-ray diffractograms. Therefore, in this paper we continue our recent investigations and characterize electrodeposited Mo–O–C–Se films. Our motivation for characterizing these films is driven by their potential as promising candidates for photovoltaic applications. To establish the suitability of these thin films as a photovoltaic material, it is essential to study the distribution and nature of compounds present in the deposits and their optical properties.

2. Experimental

A commercially available ISE-2 three-electrode system with a PI-1-50 potentiostat coupled to a PR-8 programmer (ZIP, Russia) was adopted to deposit thin films on commercially available SnO_2 coated glass plates. The thickness of the SnO_2 layer was 1 μm and the sheet resistance was 292 Ω/cm^2. A plate was fixed in a stainless steel cylindrical holder, and a copper stick served as the contact. The working area of the SnO_2 plate was 4.5 cm^2. The conducting SnO_2 coated glasses were cleaned with acetone and then cleaned chemically in 0.1 M HNO_3, rinsed with distilled water and dried. A standard $KCl_{(sat)}$|AgCl, Ag electrode was used as the reference electrode. A platinum wire with the diameter of 1.0 mm and the active surface area of 12.5 cm^2 was used as the counter electrode.

Electrolyte solutions, pH = 8.3, containing H_2SeO_3 of fixed concentrations (0.0005 M), Na_2MoO_4 (0.05 M) and sodium citrate (0.22 M) were employed. The chemicals used were $Na_2MoO_4{\cdot}2H_2O$, H_2SeO_3 and $Na_3C_6H_5O_7{\cdot}2H_2O$, all of analytical grade. Each solution was freshly prepared with twice distilled water. The deposition was carried out at a constant potential E = –1.0 V and the deposition temperature of 15 ± 1 °C. The deposition time was 100 min. The thickness of the electrodeposited film was measured with a GAERTNER L115 laser ellipsometer (USA, Gaertner Scientific Corporation). The morphology of deposits was examined with a JOEL-SEM-1C25S (Japan) scanning electron microscope (SEM). For each sample, 10 surface points were examined.

An atomic force microscope Nanotop-206 (Microtestmashines Belarus) operating in a contact state mode was used to investigate the roughness of the surface. It used a silicon cantilever, with the force constant of 5.0 N/m. The image processing and analysis of the scanning probe microscopy data were performed using the Windows based program Surface View, Version 1.0.

X-ray photoelectron spectroscopy (XPS) and Fourier transform infrared (FTIR) spectroscopy experiments were performed to obtain information on the exact composition of electrodeposits. X-ray photoelectron spectra were obtained with a Kratos Analytical XSAM800 spectrometer. The energy scale of the spectrometer was calibrated using Au $4f_{7/2}$ and Cu $2p_{3/2}$ Ag $3d_{5/2}$ peaks. The source was operating in aluminium anode mode: non-monochromatized AlK_α with the photon energy of 1486.6 eV. The O 1s, C 1s, Mo 3d, and Se 3d spectra were determined at the 20 eV pass energy (0.05 eV energy increment) of the hemispherical analyser. The fixed analyser transmission (FAT) mode was used. The resolution of the instrument was 0.2 eV. The charging effects were corrected by referring the binding energies to that the of C 1 s line at 284.8 eV. The relative atomic concentrations of oxygen, carbon, molybdenum, and selenium were calculated from an appropriate peak area with respect to the sensitivity factors, using the original Kratos software. The XPSPEAK41 software was employed for the peak fitting procedure [7]. The Shirley background with Lorenz to Gauss rate 0:100 and a symmetric line shape for all peaks were used. Assignation of the signals to specific structures or given oxidation states of elements analysed was done by comparison with data available from the NIST standard Reference Database 20, Version 3.4 [8] and to literature references. All samples were scanned as received – without undertaking ion beam surface cleaning procedure.

Mo–O–C–Se deposits were scraped with a non-metallic scraper, and then scrapings were solid-mixed with KBr, modulated into pellets and investigated by the FTIR spectroscopy to determine the chemical structure and binding configuration of a thin film. Spectra were recorded on a Perkin–Elmer FTIR system spectrum GX with the resolution of 1 cm^{-1} in the 4000–400 cm^{-1} spectral range.

UV–Vis spectrometry was used to investigate the optical behaviour of the films. UV–Vis spectra were recorded with a UV/Visible Spectronic Genesis spectrophotometer in the range 200–800 nm. The absorption spectra of thin films were recorded using an identical transparent tin oxide coated glass plate as a reference, and the values of the optical absorption coefficient α were not corrected for the reflectance from the film surface. The optical bandgap energy, E_{og}, was obtained by studying the absorption edge behaviour.

3. Results and discussion

3.1. XPS analysis

The composition of deposits has been determined by the XPS measurements. The recorded Mo 3d, Se 3d, O 1s and C 1s core level (CL) spectra are shown in Figs. 1–4, respectively. The line shape of measured Mo 3d CL spectrum (Fig. 1) is highly asymmetric, indicating the presence of mixed oxidation states of Mo. The molybdenum oxidation state was estimated by deconvolution of the peaks in the Mo 3d region. The spin–orbit splitting between Mo $3d_{5/2}$ and Mo $3d_{3/2}$ signals was set to 3.14 eV and the integral intensity of the doublet peaks was fixed before the fitting procedure was run.

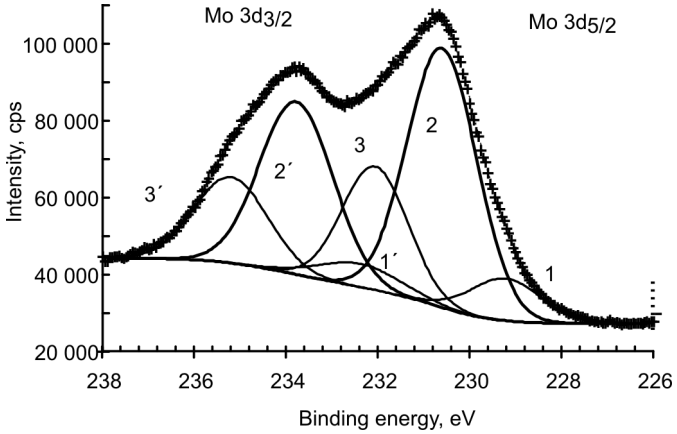

Fig. 1. Mo 3d XPS spectra from Mo–O–C–Se film electrodeposited on a SnO_2–glass plate: crosses – acquired data, dashed line – fitted curve, 1– $MoSe_2/Mo_2C$, 2 – $MoO_2/Mo_x(OH)_y$, 3 – MoO_3

Using the deconvolution technique, the best fit was obtained by resolving the spectrum into three pairs of Gaussian peaks, where 1, 2 and 3 represent the Mo $3d_{5/2}$ level of different molybdenum oxidation states. The primed peaks represent Mo $3d_{3/2}$ levels, respectively. The core level binding energy values of Mo $3d_{5/2}$ signals were compared with the values of corresponding states reported in the literature. When molybdenum is bound to selenium, the characteristic Mo $3d_{5/2}$ signal appears at E_b = 228.8 eV [9, 10]. It should be noted that the Mo $3d_{5/2}$ signal with a binding energy of 228.6 eV is typical of Mo^{2+} in Mo_2C [11, 12]. According to literature data, the energy values of the Mo $3d_{5/2}$ photoelectrons for MoO_2 and MoO_3 are ca. 229 eV [13–17] and 232 eV [13–15, 17, 18], respectively. A peak with the binding energy of 230.8 eV is midway between those Mo $3d_{5/2}$ values assigned to MoO_2 and MoO_3 and corresponds to the Mo^{5+} state associated with the mixture of oxides and hydroxides, mainly in the form of Mo^{4+} and Mo^{5+} [14, 19, 20].

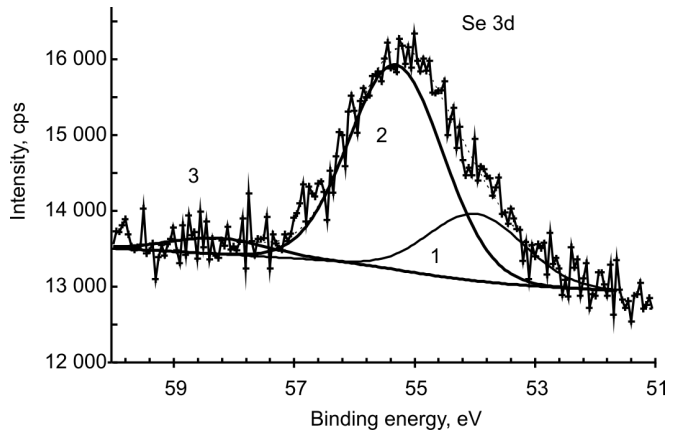

Fig. 2. Se 3d XPS spectra from Mo–O–C–Se film electrodeposited on a SnO_2–glass plate: crosses – acquired data, dashed line – fitted curve, 1– $MoSe_2$, 2 – Se, 3 – SeO_2

The Se 3d spectrum (Fig. 2) of a film sample shows the total peak envelope with the binding energy of 56 eV, which could be resolved into three peaks at 53.8, 55.9 and 58.3 eV. The Se 3d spectrum displaces the expected $MoSe_2$ peak with the binding energy 53.8 eV [21, 22]. This peak and the position of the signal from Mo $3d_{5/2}$ level at E_b = 228.7 eV strongly suggest the presence of $MoSe_2$ in thin film layers. It is known that the binding energy of elemental selenium is about 55.4 eV [22, 23]. A small peak centred at 58.3 eV indicates that the film layer may contain SeO_2 [24, 25].

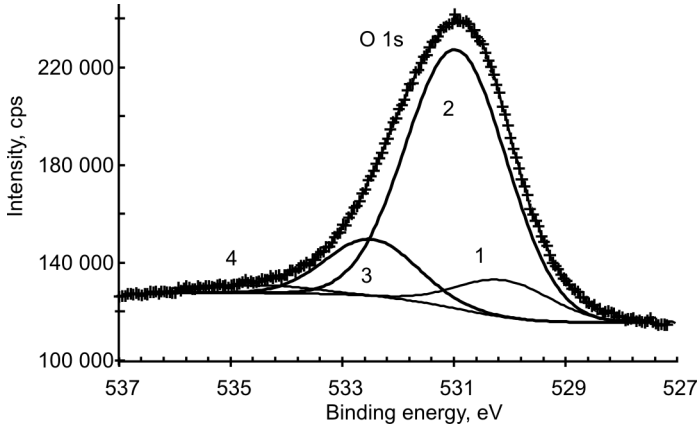

Fig. 3. O 1s XPS spectra from Mo–O–C–Se film electrodeposited on a SnO_2–glass plate: crosses – acquired data, dashed line – fitted curve, 1 – Mo–O, 2 – Mo–OH, 3 – H_2O, 4 – C=O

The O 1s spectrum (Fig. 3) can be deconvoluted into four contributions with the binding energies of 530.2, 531.1, 532.5 and 534.5 eV. The peaks at around 530 eV are known to result from oxides, and the peak at 532 eV may be assigned to the structural

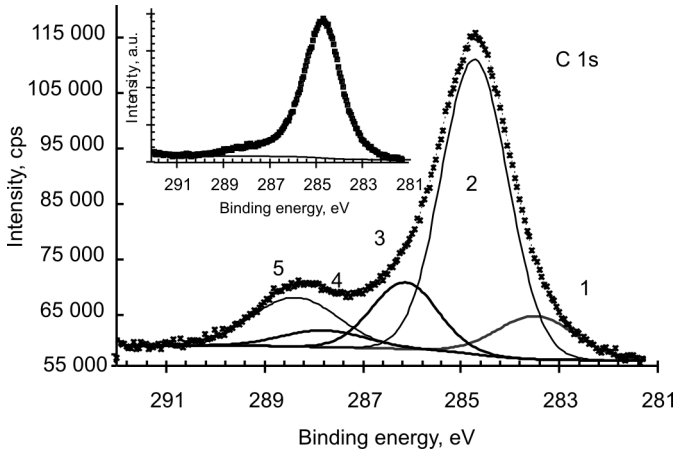

Fig. 4. C 1s XPS spectra from Mo–O–C–Se film electrodeposited on a SnO_2–glass plate: crosses – acquired data, dashed line – fitted curve, 1– Mo_2C, 2 – C–C or C–H, 3 – C–O, 4 – C=O, 5 – O– C=O. Inset: pure SnO_2–glass plate

water while the peak at 531 eV to hydroxide [17, 19]. Besides, the plot areas of peaks corresponding to oxides are small compared with the area of hydroxides. This observation suggests that the films consist largely of hydroxides. The O 1s peak component at 534.5 eV corresponds to C=O from citrate [26].

Figure 4 shows the C 1s region, after curve fitting to discriminate the various contributions. A very small peak at 283.6 eV is assigned to molybdenum carbide, in agreement with results published in the literature [15, 27]. The presence of small quantities of carbides, probably Mo_2C, has been observed in Mo–Co alloy electrodeposition from the sulphate–citrate medium [14]. The main signal at 284.8 eV corresponds to C–C and C–H bonds. Signals at 286.24, 287.88 and 288.46 eV are consistent with the presence of C–O, C=O and O–C=O groups, respectively. These bands mainly originate from the citrate ion [26]. The XPS data are summarised in Table 1.

Table 1. XPS results derived from the curve fitted deconvoluted spectra

Element	Atomic percentage, %	Binding energy, eV	FWHM, eV	NIST data	Oxidation state	Attribution to structural element found in	Relative percentage, %
Mo $3d_{5/2}$	20.81	229.2	1.8	228.3	4+/2+	$MoSe_2$. Mo_2C	10.18
		230.6	1.8	230.6	4+/5+	$MoO_2/Mo_x(OH)_y$	62.0
		232.0	1.7	232.6	6+	MoO_3	27.82
Se 3d	1.52	53.8	1.8	53.5	2–	$MoSe_2$	24.18
		55.9	1.8	55.7	0	Se	70.59
		58.3	1.9	58.0	4+	SeO_2	5.23
O 1s	60.19	530.1	2.0	530.8		Mo−O	7.14
		531.1	2.0	531.8		$Mo_x(OH)_y$	78.42
		532.3	1.9	532.8		H_2O	12.61
		533.7	2.0	535.1		C=O	1.83
C 1s	17.48	283.6	1.9	282.7		Mo_2C	10.19
		284.8	1.6	284.4		C–C, C–H	59.43
		286.24	1.6	286.4		C–O	13.33
		287.9	2.0	287.8		C=O	4.21
		288.5	2.0	289.0		O–C=O	12.84

3.2. FTIR studies

FTIR spectrum (Fig. 5) has been analysed in terms of the vibration of isolated molecular units and based on literature IR data on SeO_2 [28–31] and molybdenum oxides [32–36]. The results (cf. Table 2) strongly suggest that some selenium oxide exists in thin film layers, whereas weak absorption peaks indicate that the SeO_2 concentration is small.

The most pronounced absorption peak at 741 cm^{-1} is clearly related to Mo(IV) oxides [32–34]. The symmetric stretching modes of the terminal Mo=O bond of crystalline MoO_2 and crystalline MoO_3 appears at 985 cm^{-1} [35] and 990 cm^{-1} [36], respec-

tively. The terminal double bond peak downshift with respect to MoO_2 and MoO_3 might be assigned to the presence of OH groups in the structure of molybdenum oxide.

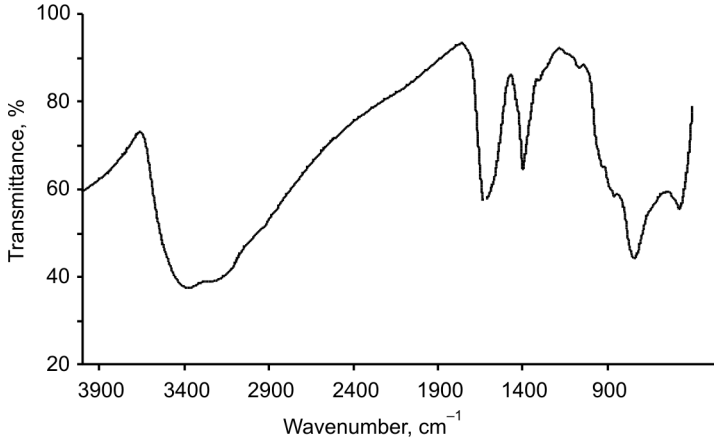

Fig. 5. FTIR spectrum of the Mo–O–C–Se film recorded in 4000–400 cm^{-1} spectral region

Table 2. Results from the analysis of FTIR spectrum of Mo–O–C–Se film

Wavenumber, cm^{-1}	Assignment
474	ν_s (Se–O–Se)
741	ν (Mo–O)
866	ν_{as} (O–Mo–O)
927	(Mo=O)
1065	(Se–O)
1398	COO^-
1621	δ (H–O–H), COO^-,
3373	ν (Mo–OH),

As a result of this interaction, a broad band assigned to the stretching mode ν_{OH} of adsorbed water molecule and OH groups linked in the form of Mo–OH is present at 3373 cm^{-1}.

3.3. Morphology of a thin film layer

Thin film layers with the thickness of 110 ± 60 nm were electrodeposited on a SnO_2–glass plate. Visually, the as-deposited films are mirror-like and coloured in a brown tint. Thin film layers were analysed without further treatment other than rinsing with distilled water. The micrograph of a thin film layer shown in Fig. 6 indicates

long-sized wires distributed all over the surface. AFM images (Fig. 7) show that wires cover the surface well, without any cracks and pinholes.

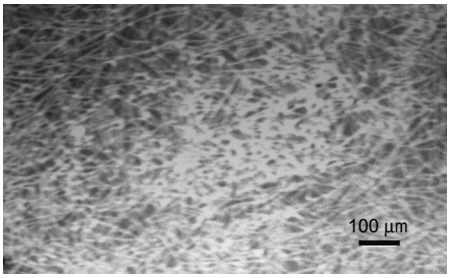

Fig. 6. SEM image of the Mo–O–C–Se film electrodeposited on a SnO_2–glass plate

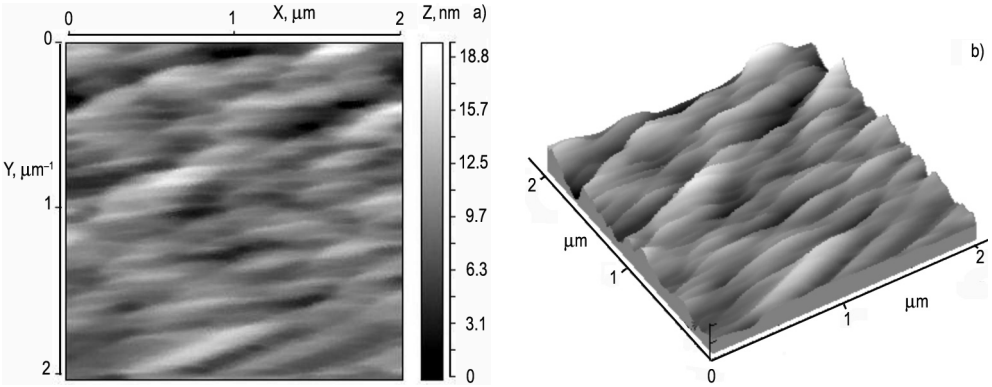

Fig. 7. AFM images of the Mo–O–C–Se film electrodeposited on a SnO_2–glass plate; a) 2D topography, b) 3D topography

3.4. UV–Vis studies

The optical absorption of the film was studied in the wavelength range from 200 to 800 nm without accounting for reflection and transmission losses. The UV–Vis transmittance spectrum of freshly deposited thin Mo−O–C–Se film is shown in Fig. 8. The transmission shows an intense minimum in the UV region. A less intense minimum in the red region is also observed. An absorption edge of the film is observed at 670 nm and lies in the visible wavelength range. Transmittance values higher than 100% between 670 and 800 nm can be ascribed to the fact that the Mo–O–C–Se film surface is smoother and less light-scattering than the SnO_2 surface used as a reference for optical transmission measurements.

The optical absorption coefficient α for the wavelength range near and below the absorption edge is found to have a value of 3.98×10^4 cm^{-1}. The variation of optical density with wavelength was analysed to find the nature of transition involved and the optical bandgap energy (E_{og}).

The variation of the optical absorption coefficient α near the absorption edge follows the power law in the form

$$\alpha = \frac{B(E - E_{og})^n}{E} \tag{1}$$

where: E is the photon energy, $h\nu$, E_{og} is the bandgap energy of the system, B is the function of the density of states near the conduction and valence band edges. The value of n is 2 for allowed direct transition and 1/2 for the allowed indirect transition.

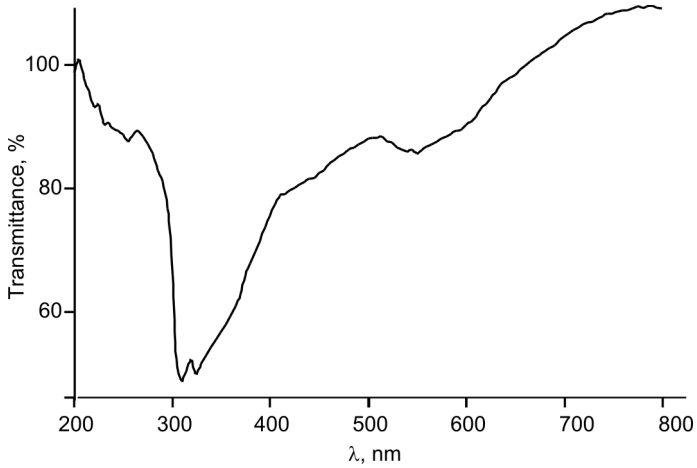

Fig. 8. UV-Vis spectrum of the Mo–O–C–Se film electrodeposited on a SnO_2–glass plate

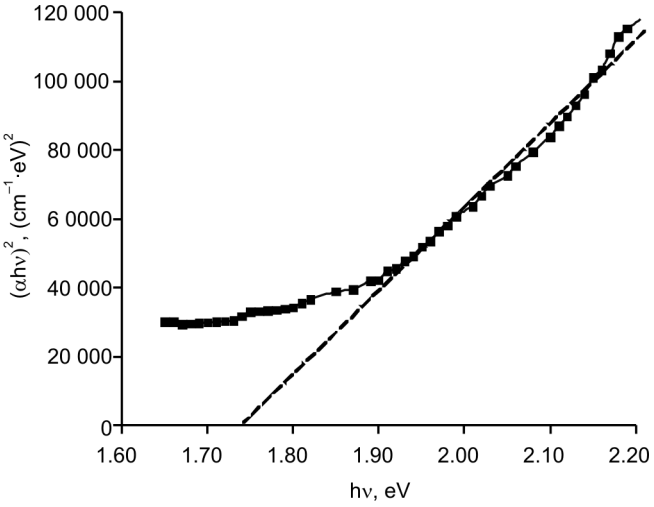

Fig. 9. Plot of $(\alpha h\nu)^2$ versus photon energy of the Mo–O–C–Se film electrodeposited on a SnO_2–glass plate

High α values suggest the existence of direct bandgap transition. The type of optical transition in the Mo–O–C–Se film has been determined from the dependence of $(\alpha h\nu)^2$ on the photon energy (Fig. 9). A linear rise near the absorption edge confirms the direct nature of transition. Extrapolating the linear part of the plot towards zero absorption, the intercept with the energy axis determines the optical bandgap energy (E_{og}) value of 1.75 eV.

4. Conclusions

XPS analysis confirms that Mo–O–C–Se film layers are heterogeneous and are composed of $MoSe_2$, Se, SeO_2 and molybdenum oxides and hydroxides. XPS core level analysis revealed the presence of Mo^{4+}, Mo^{5+} and Mo^{6+} oxidation states.

FT-IR spectra confirmed the hydrous nature of Mo–O–C–Se film.

SEM and AFM revealed the film surface to be of device-grade quality, and to be free of any pinholes.

Optical studies showed that thin Mo–O–C–Se film has a high optical absorption coefficient and direct band to band type optical transition. The bandgap energy E_{og} equals 1.75 eV.

References

[1] BOLIVAR H., IZQUIERDO S., TREMONT R., CABRERA C.R., J. Appl. Electrochem., 33 (2003), 1191.
[2] BEATO P., BLUME A., GIRGSDIES F., JENTOFT R.E., SCHOEGL R., TIMPE O., TRUNSCHE A., WEINBERG G., BASHER Q., HAMID F.A., HAMID S.B.A., OMA E., MOHOD SALIM L., Appl. Catal. A, 307 (2006), 137.
[3] US Patent No. 6214090, 2005.
[4] YUFIT V., NATHAN M., GOLODNITSKY D., PELED E., J. Power Sources, 122 (2003), 169.
[5] NAGIRNYI V.M., APOSTOLOVA R.D., BASKIEVICH A.S., SHEMBEL E.M., Russ. J. Appl. Chem., 76 (2003), 1438.
[6] DUKSTIENE N., TATARISKINAITE L., Polish J. Chem., 80 (2006), 1715.
[7] XPSPEAK41 software, http://www.phy.cuhk.edu.hk/~surface/ , April 2005.
[8] National Institute of Standard and Technology, NIST on line Databases. X-ray Photoelectron Spectroscopy Database. http://www.sr.data.nist.gov/xps (Accessed March 2007)
[9] GRIM S.O., MATIENZO L.J., Inorg. Chem., 14 (1975), 1014.
[10] BOLIVAR H., IZQUIERDO S., TREMONT R., CABRERA C.R., ASSMANN L., BERNEDE J.C., DRICI A., AMORY C., HALGAND E., MORSLI M., Appl. Surf. Sci., 246 (2005), 159.
[11] ZHANG Y., XIN Q., RODRIQUEZ-RAMOS I., GUERRERO-RIUZ A., Mat. Res. Bull., 34 (1999), 145.
[12] BRIGGS D., SEAH M.P., *Practical Surface Analysis*, Vol. 1, Wiley, New York, 1990.
[12] ZACH M.P., INAAZU K., NG K.H., HEMMINGER J.C., PENNER R.M., Chem. Mater., 14 (2002), 3206.
[14] GOMEZ E., PELLICER E., VALLES E., J. Electroanal. Chem., 580 (2005), 238.
[15] RUIZ F., BENZO Z., QUINTAL M., GARABOTO A., ALBORNAZ A., BRITO J.L., Appl. Surf. Sci., 252 (2006), 8695.
[16] DI G.G.D., SELMAN J.R., J. Electroanal. Chem., 559 (2003), 31.
[17] BARTOLOME J.F., DIAZ M., REQUENA J., MOYA J.S., TOMSIA P., Acta Mater., 47 (1999), 3891.
[18] PATISSIER-BLONDEAU V., DOMENICHINI B., STEINBRUN A., BOURGEOIS S., Appl. Surf. Sci., 175 (2001), 674.

[19] NAKAYAMA M., KOMATASU H., OZUKA S., OGURA K., Electrochim. Acta, 51 (2005), 274.
[20] SANCHES L.S., DOMINIGUES S.H., MARINO C.E.B., MASCARO L.H., Electrochem. Commun., 6 (2004), 543.
[21] BASOL B.M., KAPUR V.K., LEDIDHOLM C.R., MINICH A., HALANI A., First WCPEC, Dec. 5–9, 1994, Hawaii.
[22] SALTAS A., PAPAGEORGOPOULOS C.A., PAPAGEORGOPOULOS D.C., TONTI D., PETTENKOFER C., JAEGERMAN W., Thin Solid Films, 389 (2001), 307.
[23] SURODE P.R., RAO K.J., HEGD M.S., RAO C.N.R., J. Phys. C, 12 (1979), 4119.
[24] DIMITRIEV Y., YORDANOV ST., LAKOV L., J. Non-Crystal. Solids, 293 (2001), 410.
[25] IWAKURO H., TATSUYMA C., ICHIMURA J., Appl. Phys., 21 (1982), 9463.
[26] CHONGDAR S., GUNASEKARU G., KUMAR P., Electrochim. Acta, 50 (2005), 4655.
[27] LECLERCQ G., KAMAL K., LAMONIER J.F., FEIGENBOUM L., MALFOY P., LECLERCQ L., Appl. Catal. A, Gen., 121 (1995), 169.
[28] NAKAMOTO K., IR *Spectra of Inorganic and Coordination Compounds*, Mir, Moskva, 1991 (in Russian).
[29] SIMON A., PACTZOLD R., Anorg. Allg. Chem., 301 (1959), 246.
[30] BRABSON G.D., ANDREWS L., MARSDEN C., J. Phys. Chem., 100 (1996), 16487.
[31] CHEN Y.-W., LI L., D'ULIVO A., BELZILE N., Anal. Chim. Acta, 577 (2006), 126.
[32] NIU Z.J., YAO S.B., ZHOU S.M., J. Electroanal. Chem., 455 (1998), 205.
[33] GOMEZ E., PELLICER E., VALLES E., J. Appl. Electrochem., 33 (2003), 245.
[34] MELTS G., LINSEED CH., GOTTSCHALK R., DIETER M., FIND J, HEREIN D., JAEGR J., UCHIDA Y., SCHOLL R., J. Mol. Catal. A, 162 (2000), 463.
[35] MARTOS M., MORALES J., SANCHES L., J. Mater. Chem., 12 (2002), 2979.
[36] DU X., DONG L., LI CH., LIANG Y., CHEN Y., Langmuir, 15 (1999), 1693.

Received 20 November 2008
Revised 19 June 2009